Renewable Energy 223 (2024) 120012

Contents lists available at ScienceDirect

Renewable Energy

journal homepage: www.elsevier.com/locate/renene

Repairing ribbon bus bar interruptions in photovoltaic modules using non-intrusive interruption location

Félix G. Rosillo [a,*], Maria Beatriz Nieto-Morone [a,b], Josue Benavides Esteva [a,1], Felipe Soriano [a,2], Sergio Temprano [a,2], Claudia González [a], María del Carmen Alonso-García [a]

[a] Departamento de Energía, Unidad de Energía Solar Fotovoltaica, CIEMAT, Av. Complutense, 40, 28040, Madrid, Spain

[b] ETSIAAB, LPF-TAGRALIA, Universidad Politécnica de Madrid, Av. Puerta de Hierro, nº 2, 28040, Madrid, Spain

ARTICLE INFO

Keywords:
Photovoltaic module
Repairing
Ribbon bus bar
Tone tester
Current detector
Backsheet

ABSTRACT

Ribbon bus bar interruptions in photovoltaic modules represent approximately a 10 % of photovoltaic module failures. The purpose of the present work is to repair this failures using the simplest, fastest and cheapest techniques. Twin and single intercell interruptions are defined. The first one, twin intercell interruptions, cut off electrical current flow between two cells while the second one permits current flow between cells through just one ribbon bus bar at the cost of module efficiency reduction. We propose non-intrusive methods to find precise location of single and twin intercell interruptions. A simple technique for intercell interruption repairing is described. Three modules were repaired, multiplying its power production in two cases by 4, when comparing with its non-repaired power production. The third module did not produce any electricity before repairing, and after being repaired produced a power similar to its nominal value. The proposal of repairing can be put into practice in modestly equipped factories and laboratories, without using expensive and time consuming techniques.

1. Introduction

Due to the exponential increase of PV, waste generation and scarcity of natural resources are becoming important problems in the growth of solar photovoltaics [1–4]. The scientific community is seriously analyzing and proposing solutions to these problems. Recent studies show that the quantity of waste generated by discarded PV modules (M. B. [5]), compromises the sustainability of this type of energy, both for reasons directly related to the environment and to the depletion of raw materials [1].

Usually, manufacturers of photovoltaic modules provide a warranty of at less 25 years of operation for their products [6,7]. However, in some cases, solar PV modules are removed from operation because they do not work properly or do not meet the user's expectations, with a total or partial loss of their power generation capacity ((M. B. [5])). The time during which the solar module has worked can be considered as its end of life. In some cases this end of life can be an objective data, as for example in the case of modules destroyed by a fire, while in other cases the end of life is more subjective data, depending on the user. For example a reduction in power output may (or may not) be accepted by some users, and evidence of backsheet degradation may (or may not) by accepted by others.

Module failure analysis is gaining increasing interest due to the trend towards circularity in all technologies. There is an extensive literature classifying the different causes that can reduce power production or generate safety issues in solar modules. A wide variety of failures can be mentioned [8], such as glass breakage, frame breakage or detachment, connector failure, connection box degradation with high temperature generated in the electrical contacts, degradation of the union of the box to the backsheet, yellowing, intercell connection failure, broken or cracked cell, delamination. The quick connectors can be also a source of trouble if the electrical contacts are poor, as this fault is the origin of fires

* Corresponding author.

E-mail addresses: f.rosillo@ciemat.es (F.G. Rosillo), MariaBeatriz.Nieto@ciemat.es (M.B. Nieto-Morone), josue.benavidese@imre.uh.cu (J.B. Esteva), felipe.soriano@atisistemas.com (F. Soriano), sergiotemprano@hotmail.com (S. Temprano), claudia.gonzalez.itaca@gmail.com (C. González), carmen.alonso@ciemat.es (M.C. Alonso-García).

[1] Permanent address: Universidad de la Habana, Instituto de Ciencia y Tecnología de Materiales, Laboratorio de Investigaciones Fotovoltaicas. 4JM8+4V4, Zapata, La Habana, Cuba.

[2] Worker from ATI Sistemas company subcontracted by CIEMAT.

https://doi.org/10.1016/j.renene.2024.120012
Received 31 August 2023; Received in revised form 14 December 2023; Accepted 11 January 2024
Available online 14 January 2024

in PV installations. Bypass diode failure can result in the loss of produced power, but also the increase of negative effects such as hot spots and, consequently, PV module degradation. ([8–10] (M.A. [11])). Some of these failures, such as yellowing, do not seriously threaten the operability of the module, while others, such as backsheet degradation, reduce the functionality, safety, or directly lead to the end of the lifetime of a solar module.

Many works are being performed in the recyclability of PV modules and in the economic competitiveness of each process [3,4,7,12–14]. However there is not much work on the repair of PV modules [15–18, 26]. Paradoxically, one of the reasons for the success of PV -the dramatic reduction in W_p prices-is making this energy source less sustainable: The price of a new PV module is so low that from an economic point of view, repairing PV modules do has just a marginal interest. If the focus is on environmental sustainability and reducing environmental impact, then repairing PV modules and extending their operative lifetime must be a priority. In our opinion, government legislation must set up political and economic scenarios that boost the repair of PV modules [7,19,20].

In this paper we propose some techniques for locating and repairing a particular and frequent source of reduction in PV module energy production: ribbon bus bar interruption between cells. This type of failure accounts for 10 % of the module failures [8]. The techniques proposed for fault location and repair techniques are very easy to perform, even in non-specialized laboratories or factories. In particular, fault location avoids punching and damaging the module backsheet. While we have used expensive and time consuming techniques routinely used in PV laboratories (such as electroluminescence (EL)) and IV curve measurement) to support our findings and proposals, simple techniques developed for fauld location and repair (especially fault location) can be performed without many resources.

In two previous papers [15,21], ribbon bus bar interruptions were repaired. One of the papers [15] used two methods: One consisting of complete backsheet removal, change of busbar and finally placement of a new backsheet. The other method is a simplified method, consisting of repairing locally the interruption by removing the backsheet in the repairing area, soldering the bus bar and sealing using silicone resin. The second paper [21], uses an induction heating system solder and is used in modules specifically designed for the experiment, not in modules purchased in the market and recovered from a real photovoltaic installation after failing.

With reference to backsheet repairing, a team of researchers presented several papers [16–18] where they apply flowable silicone in order to seal module backsheet.

2. Methodology

2.1. Sample description

The solar modules used in this work are three City Solar PQ 200, with the following nominal characteristics, according to their technical data sheet: Maximum power 215 W, short circuit current 7.90 A and open circuit voltage of 37.10 V. They have 60 polycrystalline cells of 156 × 156 mm manufactured by Q-Cells, their glass is 3,2 mm thickness. Three bypass diodes prevent polarity inversions. The modules measure 1.660 × 990 × 50 mm and the weight is 21 kg.

Although we do not know the exact age of the modules, we found this model was manufactured as soon as 2006 [22]. The modules have been acquired from a Photovoltaic services provider company in Spain, and are likely to have come from a repowering process of a PV installation.

After an initial characterization described in section 2.2 we selected 3 modules out of more than twenty, whose main data are shown in Table 1. The table also includes the number of interrupted ribbon bus bar and some comments. Fig. 1 shows the specific interconnections that failed in the samples. A certain "preference" for some particular spots can be observed.

2.2. Initial characterization and selection of modules: measurement of IV curve, EL and dry and wet leakage current test

In order to characterize and select the modules to be repaired an initial set of measurements is performed: dry and wet insulation tests, indoor IV curve measurement and electroluminescence (EL) measurement. Once the selected modules have been repaired, the IV curve, EL and insulation tests are repeated to evaluate the repair process.

The solar simulator used for the measurement of the IV curves is a Pasan class AAA pulse simulator. The modules were measured as close as possible to standard test conditions (STC), and additionally mathematical corrections are made so that the IV curves in this paper are supplied in STC.

Electroluminescence images are also acquired prior and after repair. The EL camera used is a Raptor Owl 640 II, 640 × 512 Pixels, 15 μm × 15 μm Pitch equipped with a Kowa LM25HC-VIS-SW 1″ 25 mm 12 MP VIS-SWIR lens. The modules are connected to a DELTA ELEKTRONIKA power supply SM 70 V-22 A, and are fed with approximately the short-circuit current of each module, as previously determined during the IV curve measurement.

It is important to clarify that it is not possible to obtain EL images from a module affected by twin ribbon bus bar interruptions. If current tries to flow between solar panel contacts, connected to a power supply and two of the cells are affected by a total ribbon bus bar interruption, the current will not flow and consequently, it will not be possible to obtain the EL image. Note that in this case, when a module in darkness is connected with a power supply, no cell or series of cells are activated by the light of the sun or solar simulator and no voltage appears that could eventually provide an alternative path to the current through the diodes. The procedure in these cases is to remove the diodes (to facilitate the access to the contacts), determine with a voltmeter which contacts of

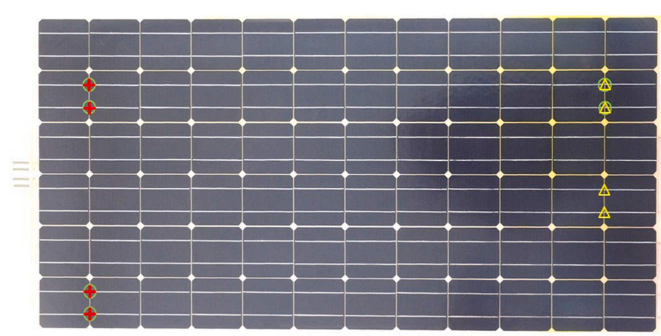

Fig. 1. Map of interruption detected in the three samples.

Table 1
Basic information about the modules used in this work. We designate modules as M1, M2 and M3.

Module (SN)	N^O of ribbon bus bar interrupted	Comments
M1 (30334814)	4	-
M2 (30894014)	6	Two of the ribbon interruptions were detected after repairing the other four ribbon interruptions
M3 (30641314)	4	The IV curve could not be measured before repairing the interruptions

solar module show voltage and apply the direct current between these contacts. In the case of the pre-repair EL images, only the active series of cells are visible to the camera, and their condition (for example cracks, etc.) can be observed. When the module is repaired, the EL image reveals all cells and it is possible to know their actual state [8].

Safety must be an important objective when repairing PV module, and any repaired module that does not pass some basic safety tests, must be decommissioned and recycled. Consequently, dry and wet insulation tests have been carried out in accordance with UNE-EN IEC 61215–2:2021. The main equipment used is a Chroma AC/DC/IR HIPOT TESTER model 19052. Additional minor equipment is used for the wet test, as a mean of achieving the appropriate temperature of the water and a container to set the required humidity conditions [23].

The initial characterization of the modules permitted to select three of the modules that showed a positive result in the wet and dry insulation test and a reduction in the power generation capability (IV curve). This was supplemented by the measurement of voltage at the contacts of the module junction box and the using EL. Both procedures show the series of cells that are still functioning. Although more than twenty modules were submitted to these tests, only three modules that comply this requirement where randomly selected.

The measurement of the IV curve before and after the reparation allowed us to obtain the percentage of power that was recovered. The EL measurement permits to check if additional damages are suffered during repair and to compare the EL image before and after repair.

In the case of the wet insulation tests, it was discovered that one of the modules did not pass the test after repairing (module M2). In order to find the source of the problem, partial insulation checks were performed: Moisture was applied successively and alternatively to aluminium frame, junction box and repair spots. This permitted to identify and repair the cause of insulation failure, which in this case was the module junction box that was separated from the backsheet, probably during manipulation for repairing. After applying additional silicone to the junction box/backsheet interface, the module passed the conventional wet insulation test.

Fig. 2 shows a flow chart of the sequence described including further steps that will be described later.

2.3. Locating the breakdown

As stated in the introduction the purpose of this work is to locate and repair ribbon bus bar interruptions in a way as simple, cheap and fast as possible. Two cases can be distinguished, twin ribbon bus bar interruptions and partial ribbon bus bar interruption between cells:

2.3.1. Twin ribbon bus bar interruptions between two cells

If some of the cell series of solar modules do not supply power, this will be reflected in a reduction in voltage when compared with previous measurements or with the nominal V_{oc} value. In the case of the modules used in this work, with three diodes and four electrical contacts in the junction box, the number of cells affected will be a multiple of 1/3 and, consequently, the module V_{oc} will be reduced accordingly. This measurement is a fast and cheap symptom requiring only the use of a voltmeter. A possible cause of this reduction in V_{oc} is a total ribbon bus bar interruption between one or more cells. This is what we call twin ribbon bus bar interruption. In this case, in well-equipped laboratories, electroluminescence fails to show the affected cells, just because no current con flow through them. By removing diodes from the junction box and checking the electrical connections between the different terminals in the junction box at the time of the EL measurement, it is possible to obtain images of non-affected series of cells, as described previously.

The method described in the literature for finding discontinuities in the electrical circuit of a PV module is to drill the back-side to locate the exact point of the failure [15]. This method is also used by a repair company (private communication). We propose a simpler and nondestructive way for finding the precise spot of the interruptions, by using a

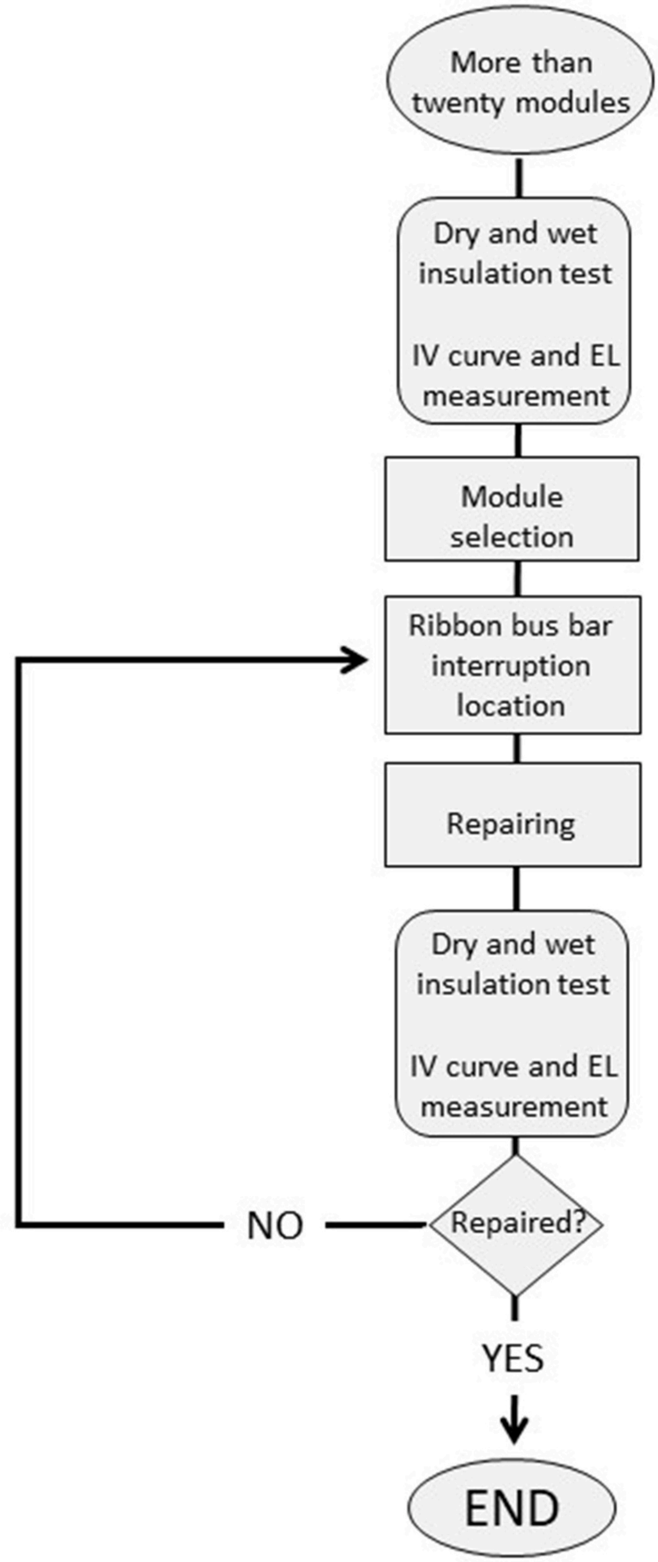

Fig. 2. Flow chart describing successive steps performed in the present work.

tone tester. Tone testers or cable locators are electrical tools, mainly used for tracing communication cabling, checking cable continuity, etc. Depending on the complexity of each particular tool, some other functions may be added to those mentioned. Tone testers consist of a voltage generator called tone generator or transmitter, connected to the cable under test (the other terminal of the tester can be connected to another cable, to earth, to an aluminum frame in the case of PV modules, etc., depending on the particular application). This tone generator or transmitter induces a modulated electrical signal in the cable under test, with its corresponding electromagnetic field. The tone generator does not introduce any current into the circuit, and the voltage signal is more or less a sawtooth signal with root mean square (RMS) values from 0.5 V to 5 V (depending on the equipment) and radio frequencies around 1000 Hz (Fig. 3). The equipment includes an antenna, receiver or sensor (for example a receiver coil), capable of detecting the electromagnetic field. The voltage induced in the receiver is converted into an audible signal. Changes in the intensity or frequency of the signal, reveal some change in the propagation of the signal introduced into the conductor by the tone generator. In our case, the interesting point is the capability of this tool to detect the interruption of intercell connections.

The market offers an abundance of instruments with similar basic purposes, but varying capabilities and characteristics. There are plenty of references on the internet for manufacturing homemade transmitters [24]. The prices range from few more than two tens of euros to even thousands of euros. In our case we worked with two different models, one of the cheapest range (25 €) and the other with a price close to 200 €. While both works quite well for the purpose, the cheapest model showed a superior performance, making easier to detect interruptions, probably due to the characteristics of the sound emitted for the receiver (a more "dirty" sound that facilitates to identify changes in the voltage signal propagation in the ribbon bus bar). The devices used are the NIMO electronic TES011 and the Fluke Networks PRO3000F50-KIT.

The practical operation of this type of device consists of connecting one of the cables of the tone tester transmitter to one of the cables that extracts energy of the solar module. The other cable of the tester is connected to the aluminum frame of the solar module, and the module itself must be isolated from the ground, furniture or other equipment. We use some chipboard pallet with good result. To improve the signal, it is recommended to situate the module at less at 500 mm of distance from the ground. The module is placed with the active cells face up. The tone detector tracks the signal in ribbon bus bar as shown in Fig. 4, generating an audible noise. When the noise disappears or reduces its intensity, it is possible that the intercell connection is interrupted.

After connecting the tone tester to the first contact, the sensor or receiver is moved along the ribbon bus bar at a small distance from the module surface or even touching the module glass. If a reduction or change in the sound emitted for the receiver is detected, it is checked by changing the initial intensity of the sound (usually the sensor incorporates some knob for this purpose). It is recommended to reduce the intensity to the lower audible level, near the hearing threshold. A quiet room is the best place for performing this task and on the contrary performing this task in the open air makes things much more difficult, due to parasitic sound. In the case of two ribbon bus bars in each cell (or more ribbon bus bars, for cells with more than two ribbons bus bars), the same procedure applied to the remaining ribbon bus bar, must supply the same results. Single interruptions in a cell are undetectable with this procedure, because if just one ribbon bus bar is broken, it receives the tone tester transmitter electrical signal from opposite directions, hiding ribbon bus bar breakage. The reason is that the two ribbon bur bars of each cell are connected at the extreme ends on the solar module by string interconnection ribbons (see for example Fig. 5: Bus bars of horizontal series of cell are conned on the right and left).

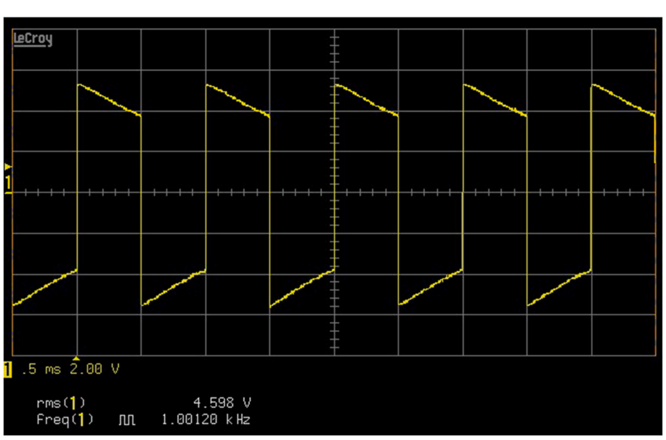

Fig. 3. Voltage waveform of one of the tone generator transmitters used in the present work.

Fig. 4. Location of twin ribbon bus bar interruptions using tone tester and taking module frame as electrical earth. The module is isolated using pallet of chipboard between the work-table and the PV module. The operator displace the receiver sensor head following the ribbon bus bars, until finding a sound change which informs of a possible ribbon bus bar interruption.

Fig. 5 illustrate the principle of operation of the device as applied to solar modules. As can be observed in the figure, electrical tester signal propagates from cell to cell except if the two ribbon bus bar (twin) interconnections are interrupted. The case where only one ribbon bus bar interrupted will be discussed later.

The tone tester transmitter is connected successively to each of the contacts in the junction box of the module. If no interruption is detected in the series of cells nearby to the module contact under test, the tone tester transmitter is connected to the next module electrical connection and the procedure is repeated as described. Usually this procedure must be done with the four contacts of each module, because the electric signal of the transmitter is dimmed as it moves away from the contact. It is useful to note that when testing one of the module contacts, the faulty connection will also be detected in the opposite direction to its nearby module contact as shown in Fig. 6, except if there is an additional twin ribbon bus bar interruption, Fig. 7. This can help to verify the result of the test.

It is possible that after finding and repairing two intercell total interruptions, the corresponding series of cells remain disconnected from the rest of the cells of the module. After a new track of the connections of the cells with the tone testers, it may be found that there was another cell interconnection failure, hidden by the previously located and repaired interruption.

This type of situation is illustrated in Fig. 7. As explained before, it is mandatory to check all the electrical contacts with the tone tester in order to find all the twin ribbon bus bar interruptions. However some cell interruptions may remain undetected. For example, it could be

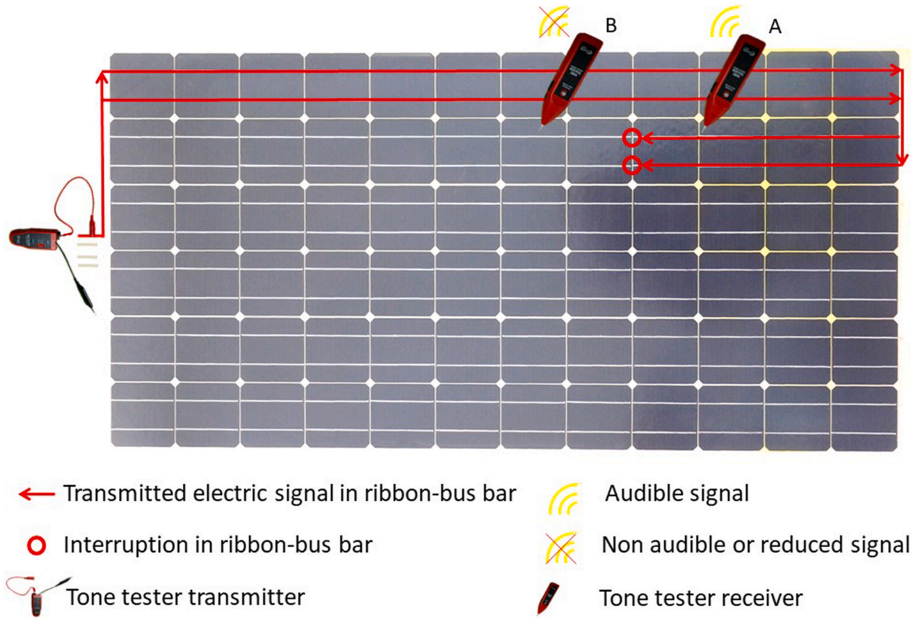

Fig. 5. Scheme of operation of a tone tester (NIMO TES011) in a PV module. On the left, tone tester transmitter is connected to module contact (red connector) and aluminum frame (black connector). At right, tone tester receiver tracks the signal in the active side of the module, by following ribbon bus bar. When the tester receiver detects the electrical signal, it emits an audible noise (A), and when the intercell ribbon bus bars (twin) are interrupted (B) the noise reduces or disappears.

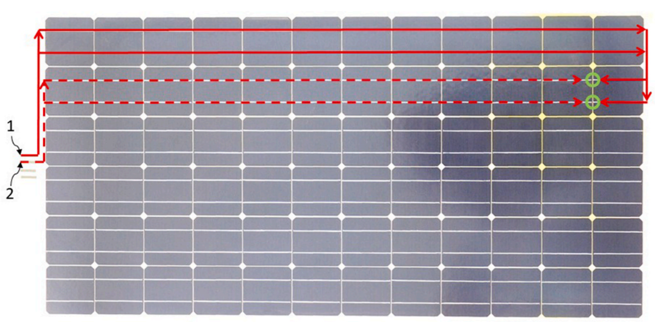

Fig. 6. Green circles show an intercell interruption that can be detected by connecting the tone tester transmitter to contact 1 in the module box and the transmitter sends the voltage signal through the red continuous arrow. Alternatively the tone tester transmitter can be connected to contact 2 in the module box and send the voltage signal through the discontinuous arrow.

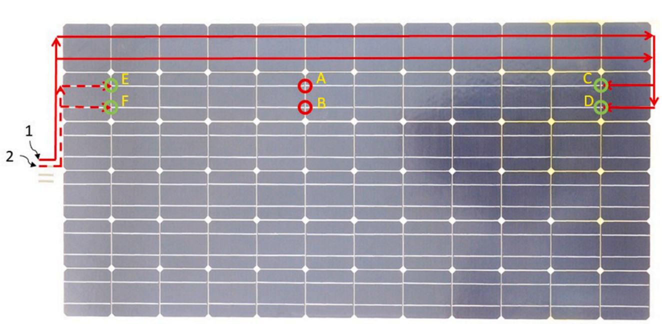

Fig. 7. Map of interruption A, B, C and D in a hypothetical module. Red lines represent tone tester electrical signal propagation and numbers 1 and 2 represent contacts in the connection box.

possible to find a hypothetical case of interruption between interconnections CD and EF. Referring to Fig. 7, both interruptions can be easily located, using contact 1 for CD and contact 2 for EF but they would make the AB interruption undetectable regardless of the terminal checked. The procedure to follow is to repair the new interruption found, and so on, if necessary.

A change in sound usually occurs in the bus ribbons that interconnect the series of cell in the extreme part of the module, where the ribbon bus bars fold twice at a 90° angle to connect to the next series of cells. In this case this does not necessarily indicate an electrical interruption, as can be determined when the signal is recovered by following the ribbon bus bar. Furthermore, it should be noted that this methodology cannot be used to check continuity on the back surface of the solar module.

The use of tone tester for this specific application, not originally designed for it, requires some self-training to understand its operation and capabilities. Nevertheless, once the operation mode is understood, it becomes an effortless and swift technique. While the process could be automatized in a repair factory, we believe the manual procedure is more appropriate when dealing with limited quantities of modules will be repaired or when automation is not an option.

Finally, it is important to remark that while EL, thermography or the use of a voltmeter permit to the revealing of possible series of cells that could be affected by twin ribbon bus bar interruptions, it is not clear which of the cells are really interrupted. To the best of our knowledge, the use of tone testers or punching are the only two techniques that permit to find the true interrupted twin ribbon bus bar, with the particularity that the punching is to some extent an aggressive technique.

2.3.2. Partial ribbon bus bar interruption between cells

Electroluminescence images reveal many cases where intercell connections are partially interrupted and the solar module appears to work correctly, with some loss of power [25]. Fig. 8 shows, by using electroluminescence (EL) images, examples of the effect of alternate interruption of the ribbon bus bar between two cells.

As can be seen in Fig. 8, partial ribbon bus bar interruptions are quite easy to identify in EL images. With reference to the repairing of this kind of failure, we consider that can be justified only when a total interruption of other series of cells force to repair the module. In our opinion, it is not justified to perform the repairing of this partial failure in a module that supply most of the power expected, due both to economic reasons and to avoid the risk of damaging de module if a failed repair occurs.

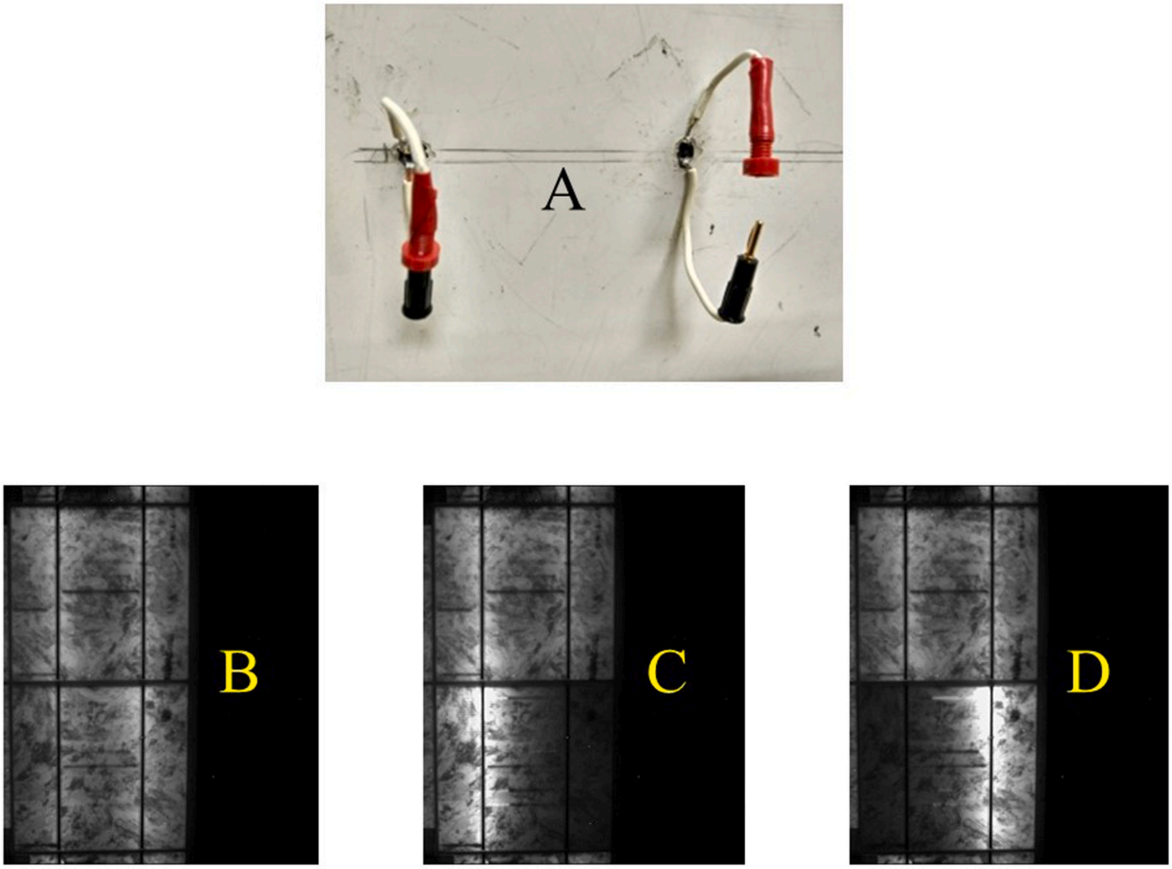

Fig. 8. Above, (A) intercell ribbon bus bar arrangement for connection and disconnection of ribbon bus bar. Below left, (B) electroluminescence with both ribbon bus bar connected. Below center, taking as reference the active face of the module (C) electroluminescence with right ribbon bus bar interrupted. Below right, (D) electroluminescence with left ribbon bus bar interrupted. Note that connected and disconnected ribbon are inverted in A.

While tone tester technique would be a desired method for single ribbon bus bar interconnection failures, it is not valid for this purpose. Fig. 9 shows an example of how the interruption would be hidden. In the image, the green circle represents a single bus bar interruption and the red arrow the electrical voltage signal generated by the tone tester transmitter. This electrical signal reaches the interruption on sides A and B. As both borders of the bus bar interruption are very close, the tone tester receiver detects a signal from both sides of the fracture, A and B. Therefore, the tester receiver is unable to distinguish the breakdown, hiding the interruption.

Where it is considered appropriate to repair single ribbon bus bar interconnection failures, the extension of the tone tester technique is desirable to avoid using of much more expensive EL or thermography images and, above all backsheet punching. In case of lack of EL and thermographic cameras, it is possible to identify ribbon bus bars that generate excessive temperature in the surface of the module glass. Fig. 10 shows an example: It illustrates temperature differences of ribbon bus bar for the cells of a series of cells of Module M2. The module is not exposed to solar irradiation, but situated in a room and connected to a DC power supply that forces a current of 7 A to flow. The temperature is measured with two thermocouples adhered to the module glass, in front of the two ribbon bus bars of each cell. The image with red border of inlet of Fig. 10, shows the measurement of two cells with thermocouples. The yellow inscriptions show ΔT between the ribbons of each cell, to be compared with their electroluminescence and thermographic images at the top of the figure. It can be seen that ΔT for cells A and B is noticeably higher than for the rest of cells, consistent with their EL and thermographic images, where brighter areas correspond to hotter ribbon bus bar temperatures. While it is not certain that this temperature difference is due to a single ribbon bus bar interruption or detachment of the ribbon bus bar, and it is important to note that neither EL nor thermographic images are enough to clarify this point. The use of thermocouple sensors provides, to this effect, similar information than EL and thermographic cameras, and consequently the decision regarding whether to repair or not is similar.

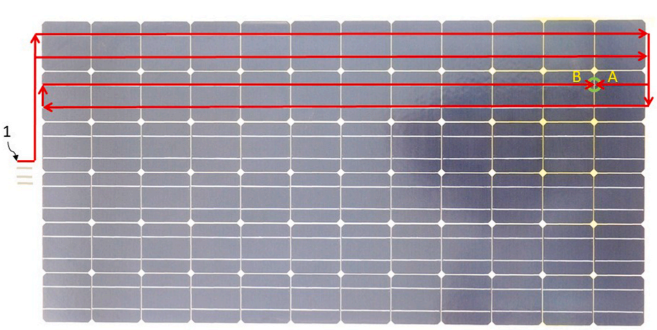

Fig. 9. Green circle represents a single interruption, situated between references A and B. Red arrow shows how the electrical voltage (not current) signal generated by the tone tester transmitter at contact 1 that can reach the interruption on both sides.

An important information to consider that justifies the tone tester failing to detect single interruption, as shown in Fig. 9, is that this device is based on voltage detection. Consequently, a current detector could help to our purpose.

Fig. 11 shows a solar panel, with a single interruption ribbon bus bar situated between references A and B, which is fed with current by a

Fig. 10. Difference of temperature of ribbon bus bar for the upper series of cells of Module M2, when a current of 7 A is flowing. A thermography is shown above, an EL image in the center and the visible image of the whole module below. The red border inlet image shows the measurement of two of the cells with thermocouple. The yellow inscriptions show ΔT between the ribbons of each cell, to be compared with their electroluminescence and thermographic images at the top of the figure.

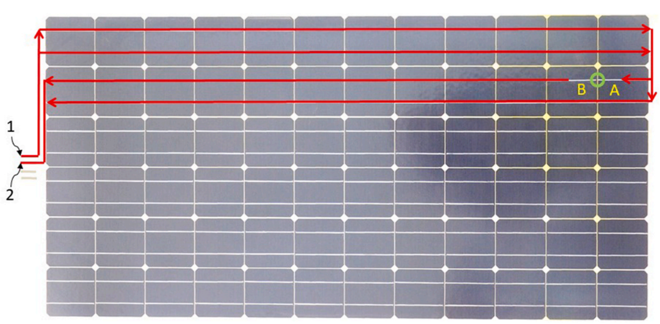

Fig. 11. Green circle represent a single interruption, situated between references A and B. Red arrow shows how an electrical current signal applied to the solar module contacts 1 and 2 can reach the interruption on both sides, but showing a decay of current at zones A and B around single interruption.

power supply. The red arrow shows how an electrical current signal applied to contacts 1 and 2 of the solar module can reach the interruption on both sides, but shows a current decay at zones A and B around the single interruption. This interval before and after the single interruption could be detected with a current detector.

We used an AC Voltage & Current detector from EXTECH instruments with a price close to 50 €. This device senses alternating current using a coil that is capable of detecting the magnetic field generated by currents greater than 200 mA. As the device does not have a tone generator, a variac or an autotransformer is used to supply AC current to the solar module from the electrical grid. Taking into account the relationship between maximum and RMS (Root Mean Square) values, $I_{RMS} = \sqrt{2}\ I_{max}$, it is recommended to use $I_{max} < I_{sc}$.

Fig. 12 illustrates the detection of a single interruption: The detector head is moved from right to left over the ribbon bus bar. In the photo number 1, the detector LEDs are on due to the presence of current. As it moves to the left, the light dims until it disappears in photos number 2 and 3. In photo 4, the LED lights up again due to the presence of current.

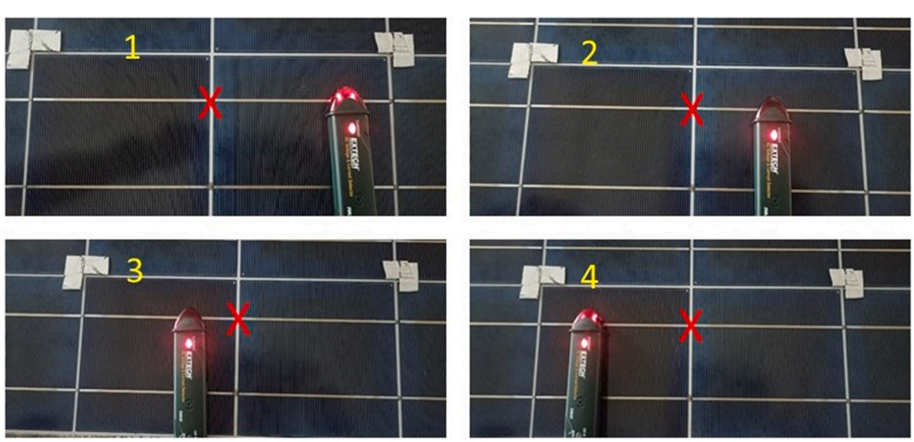

Fig. 12. Detection of a single ribbon bus bar interruption using a current detector. The red cross is the spot where the interruption is located (as shown in Fig. 8 A). The solar module is supplied with I_{RMS} = 2,82 A (3,98 A, I_{Max}). The detector was moved from right to left. In 1 and 4 the detector LEDs light due to the presence of current. In 2 and 3 the detector LEDs off reveal the absence of current.

This procedure reveals that the interconnection marked with a red cross is interrupted. When comparing with single interruptions detected in two complete solar modules using EL the coincidence is complete.

As previously mentioned, although EL, thermography or direct temperature measurement using thermocouple can be used to locate possible cells affected by ribbon bus bar interruptions, it is not clear which of the two intercell twin ribbon bus bar of each cell is actually interrupted as it can be seen in A and B of Fig. 10. For example cell A shows single intercell interruption, but it is not possible to know wheter the interruption is with the cell to its right or the cell to its left. The use of the undesired punching technique permits to select the true single interrupted ribbon-bus bar. The use of the current detector, as described before, allows to find the precise location of the spot corresponding to the single ribbon bus bar interruption.

2.4. Repairing process

Our proposal for repairing coincides in some aspects with the one of Koo Lee, particularly the use of visible light to mark the backsheet to signal the point to be repaired. The main difference is that we have not previously use backsheet punching to locate ribbon bus bar interruptions. In our opinion, this procedure could provoke future problems of permeability to exterior agents and faults in electrical insulation.

After locating of the intercell twin ribbon bus bar interruption using the tone tester, we proceed to repair the fault. We have experimented with various techniques in order to remove the backsheet and EVA to reach the interrupted ribbon bus bar. Scalpels and cutters permit to remove those layers, but it is a time-consuming task and quite risky for the cell if the operator losses control of the cutter. A special hot blade designed for this purpose can be used and also a conventional knife with soldering iron tip. In this case, it is not so easy to prevent a certain damage to the cells when trying to access to the ribbon bus bar. This procedure is somewhat similar to that of Lee's [15].

Finally we tested rotary tools, used extensively in home improvements and hobby applications. In our case we use a Dremel 4250. Rotary tools admit a huge variety of accessories. Fig. 14 shows 15 steps that we performed in order to repair bus bars. These are not fast and hard rules but the minimum steps to be done. In some cases it is necessary to repeat some steps when repairing a PV module, for example the cleaning step with the air gun.

From now on, most of the tasks will be performed using a USB microscope (Fig. 13), that permits to appreciate the details and to take photos and videos. After locating the ribbon bus bar interruption using the tone tester, it is necessary to outline the working area in the backsheet. In this working area, the drilling will be carried out that will allow access to the ribbon bus bar interruptions. A strong light, incident from the front side, helps in this task as can be seen in steps 1 and 2 of Fig. 14: In the case of a translucent backsheet, it is possible to see the work area by illuminating the front of the solar module, detecting the bus in its back and marking the area to be intervened with a pen. In cases where the backsheet is dark or not translucent, the location of the point to be drilled in the backsheet is done using 2 mm Ø cylindrical neodymium magnets, one on the front of the module and the second on the backsheet. Placing the first magnet on the module glass above the interruption (Fig. 15A) allows the second magnet to be placed on the backsheet (Fig. 15B) in the same interruption area, locating the work area and marking the area to be drilled with a pen.

Fig. 13. An USB microscope connected to a PC is used for most of the repairing steps.

Many accessories of the rotary tool where tested for our application, finding that sanding band accessories (Dremel reference 431, at 35000 rpm) are optimum for our purpose (Fig. 14.3) and permit a precise access to ribbon bus bar, eliminating backsheet and one of the layers of EVA. It is important to work delicately, to remove the backsheet and the first layer of EVA, allowing access to the ribbon bus bar without damaging the two solar cells. This task, along with all others described in the section, requires prior training on discarded modules. Additionally polishing accessories may be used (Dremel reference 429 or reference 414 at 20000 rpm) complementing the sanding process (Fig. 14.4). An air gun permits to eliminate dust and waste generated during sanding. Others accessories like bristle brush (Dremel reference 403, at 15000 rpm) help in some phases of the repairing, while rotary tools cotton accessory (Dremel reference 414 at 20000 rpm) polishes the bus bar and eliminate the remaining EVA on the surface of the bus bar (Fig. 14.4). This last step can be complemented with scalpel and air gun flow, in order to eliminate plastic remainders (Fig. 14.5).

The most delicate step appears in Fig. 14.6: Bus bar must be separated into two parts at the point of the interruption, so that a complementary piece of bus bar can be inserted (Fig. 16). Fig. 15 presents a scheme of the layout of cells, bus bars sections 1 (close to the module glass) and 2 (close to the module backsheet), the additional piece of bus bar and drops of fluid soldering. First, the bus bar section 2 is lifted and then the bus bar section 1 in Fig. 16 is lifted. For this task, a cutter and a little screwdriver are used (Fig. 14.6). The screwdriver is used to force the bus bar to fold at the selected place, taking care of not to damage the cell. The cutter is used to properly fold the bus bar. The bend helps to apply flux to the bus bar, in order to facilitate the soldering process (Fig. 14.7). A tiny drop of fluid soldering paste is applied to the extreme of the bus bar complement which is typically around 5 mm long (see Fig. 14.8). This is then inserted under the original bus bar section 1 (see Fig. 14. 9 and Fig. 16) on the active face of the solar cell (Fig. 16). Thereafter the original bus bar and the complement piece of bus bar are soldered (Fig. 14. 10) and the surplus bus bar is cut off (Fig. 14. 11). The temperature of the soldering iron tip will be around 183 °C, which is the nominal fusion value for the soldering paste used.

Finally, the new piece of bus bar receives another drop of fluid soldering paste (Fig. 14. 12 and Fig. 16), and is soldered to the original bus bar section 2 (Fig. 14.13 and 16) which is welded to the back of the cell. A continuity check using a multimeter (Fig. 14.14) or tone tester is essential before filling the hole with silicone (Fig. 14.15).

The silicone used in the present work is Dowsil 7094 a flowable sealant, that has been used before by other authors to repair PV modules [17]. This silicone is particularly fluid and can penetrate in the hole made during the repair.

The repair process described for each ribbon bus bar interruption will take from 5 to 10 min. The repairing of the complete intercell interruption (that has two broken ribbon bus bars) will then take from 10 to 20 min.

Full repair implies locating of both twin and single ribbon bus bar interruptions. While the repair of twin interruptions is mandatory, a decision is made in order wheter to repair or not to repair single interruptions. Fig. 17 shows a flow chart summarizing steps involved in

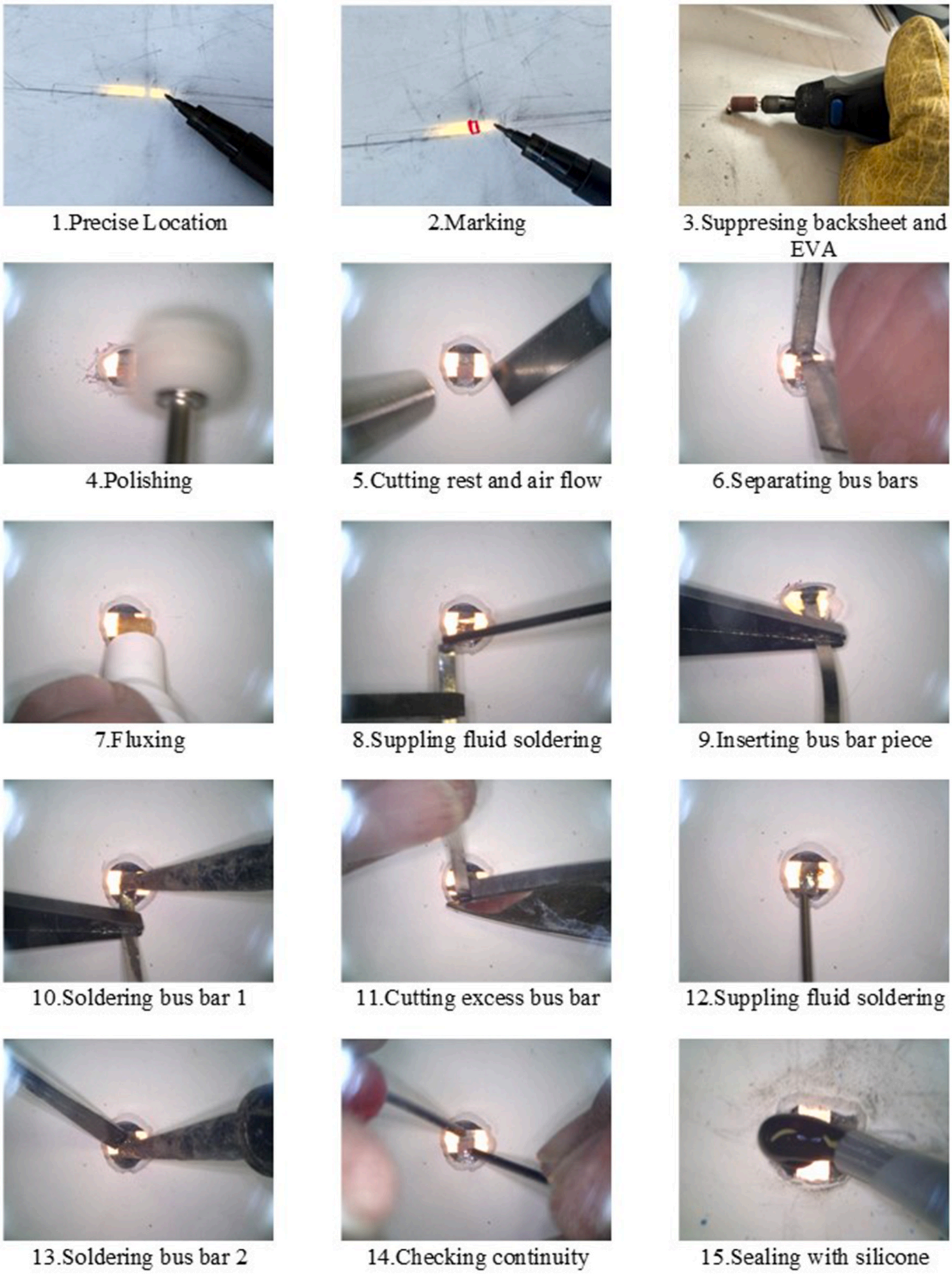

Fig. 14. Steps for repairing interrupted ribbon bus bar cell interconnection. For better illustration the sequence correspond to various ribbon bus bar repairs.

locating and repairing twin and, where applicable, single ribbon bur bas interruptions.

3. Results and discussion

Table 2 shows the maximum power values before and after repairing the PV modules. The nominal power of these modules is 215 Wp. The repairing process of M1 and M2 multiplies the generated power by 4. For module M3, which did not supply any power generation before the repair, 197,4 W is generated in STC after the repair. Figs. 18–20 show the IV and power-voltage curves of each PV module before and after the repair process. It is evident that the performance of all the modules has improved, especially for module M3 which had no energy generation before the repair.

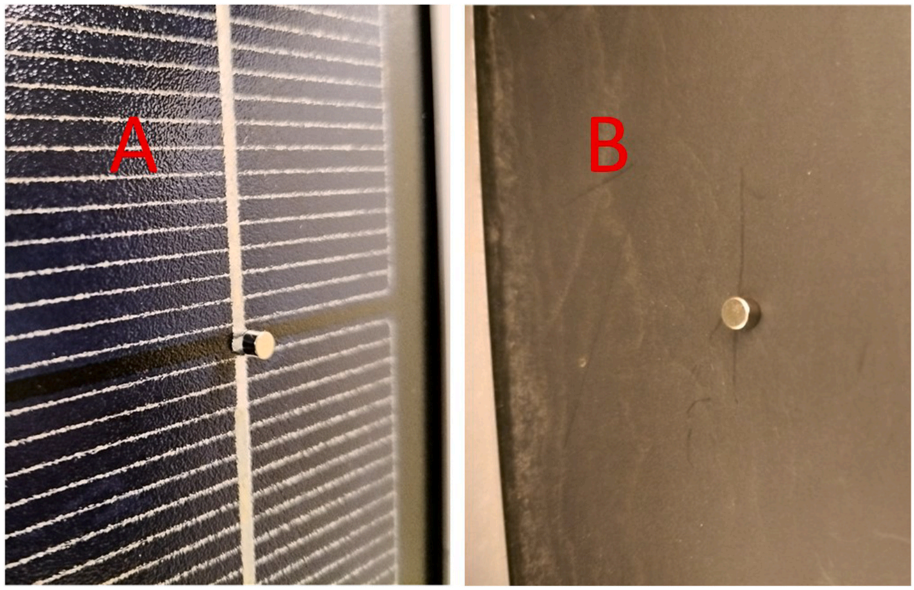

Fig. 15. Location of the point to be drilled in the backsheet of a non-translucent module, using two 2 mm Ø cylindrical neodymium magnets: A) neodymium magnet in the front of the module and B) neodymium magnet on the backsheet, magnetically coupled to magnet A).

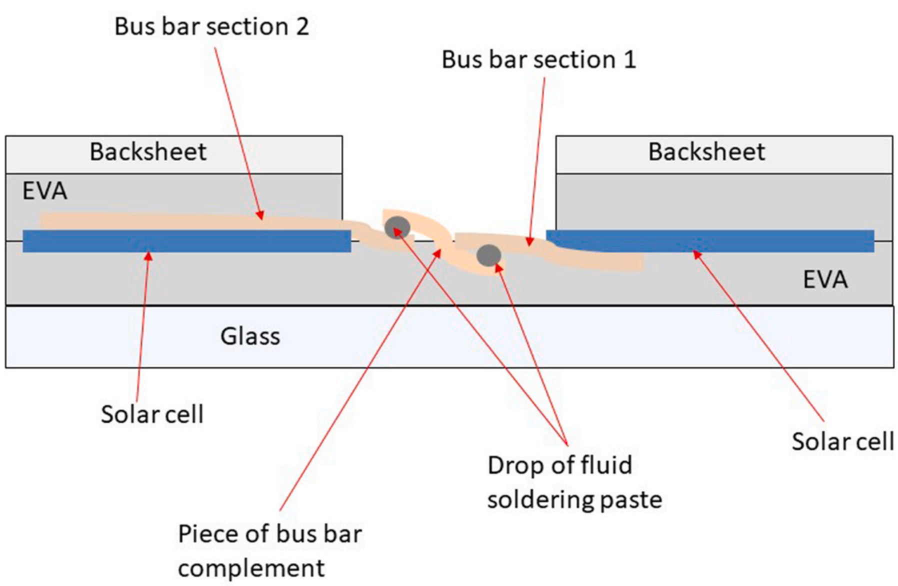

Fig. 16. Scheme of the layout of the two cells, the interrupted bus bar, the additional piece of bus bar and drops of fluid soldering.

Fig. 21 shows the EL images of each module before and after the repair. EL images reveal that for modules M1 and M2 the repaired spots do not show any signal of nearby additional ribbon bus bar interruptions. However, there are other cells in both modules in which EL images show single ribbon bus bar interruptions similar to those in Figs. 8 and 12. In the case of the M3 module, single interruptions appear next to the repaired twin interruptions as well as in other parts of the module. Modules M1, M2 and M3 amount 3 × 120 single cell interconnection and in Fig. 21 it can be observed a total of 24 single ribbon bus bar interruptions. That mean that after repairing twin interruptions they remain around a 7 % of single bus bar interruptions without repairing. Additionally, we have observed that in some cases, repairing a single interruption is followed by the interruption of the corresponding nearby bus bar connection, which requires further intervention to repair the newly interrupted connection. This and other issues will be analyzed in a future article focused on repairing single ribbon bus bar interruptions and comparing then with twin ribbon bus bar interruptions.

Repairing single interruptions could modestly increase the power production [25]. Therefore, in order to reduce the risk of damaging the modules and due to the modest gain of power, in this work, we decided not to repair the additional single interruption revealed by the current detector (fully coincident with EL images of Fig. 21).

Regarding the wet insulation test, in M3, the junction box required extra silicone because it was identified as the source of insulation failure. Following the repair, the electrical insulation was restored as described in paragraph 2.2 and all modules passed the dry and wet insulation tests.

The repair of ribbon bus bar interruptions is barely reported in scientific literature papers [15,21]. The technical skills required to the recover certain series of cells cancelled by ribbon bus bar interruptions are not difficult to obtain and the materials required are generally easily available. Usually this type of failure is detected by using combined IV

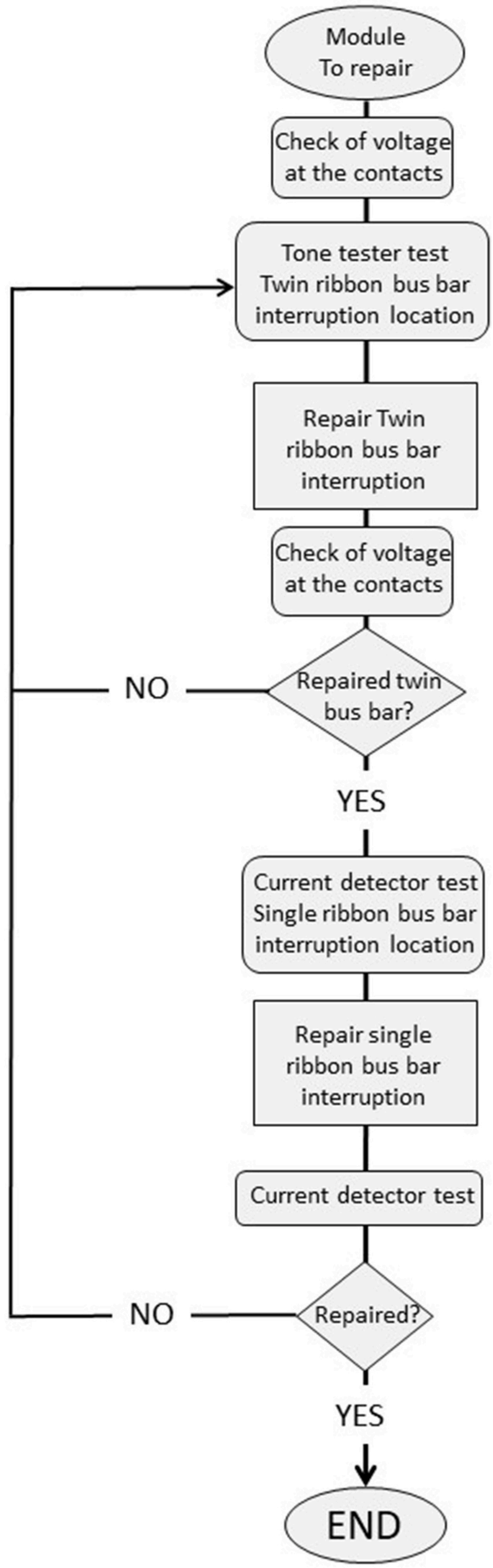

Fig. 17. Flow chart summarizing steps performed for locating and repairing twin and, if necessary, single ribbon bur bas interruptions.

Table 2
Maximum power generated before the repairing and after the repairing. Module M3 was unable to generate IV curve before repairing.

Module	P_{max} (W) Before repairing	P_{max} (W) After repairing
M1 (30334814)	51,8	199,4
M2 (30894014)	48,5	198,5
M3 (30641314)	0	197,4

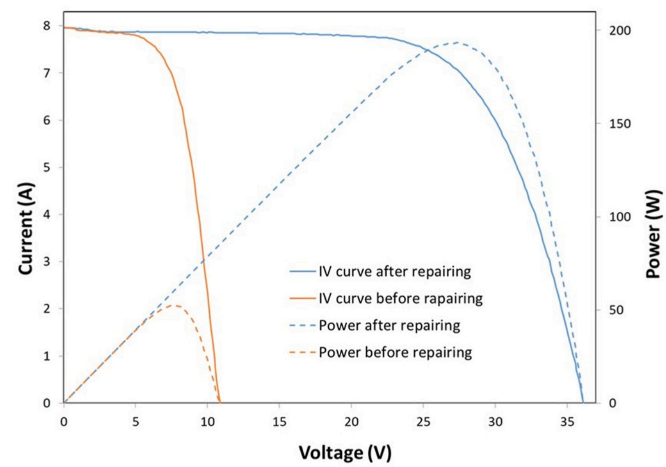

Fig. 18. Module M1 IV curves and power-voltage curves before and after repairing.

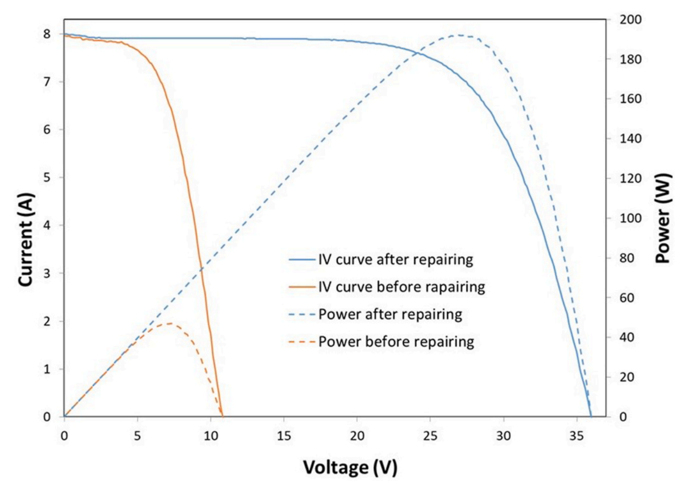

Fig. 19. Module M2 IV curves and power-voltage curves before and after repairing.

curve and electroluminescence measurements. The capabilities and equipment to perform both EL and IV curve are costly and only within reach of specialized laboratories. This paper presents a proposal for cheap and fast techniques that do not require either electroluminescence or IV curve measurement. The results obtained with these techniques have been verified with the IV and EL measurements.

The repair of twin ribbon bus bar interruptions have been documented previously [15]. These authors apply two methods, one involving the complete relamination of the module and the other, simpler, removing the backsheet and EVA only at the specific location of the bus bar interruption. While both methods used by the authors achieve their main objective, both have some drawbacks. Complete relamination of the module is not within reach of factories that do not own laminator machine. It is more time and resource-consuming than the

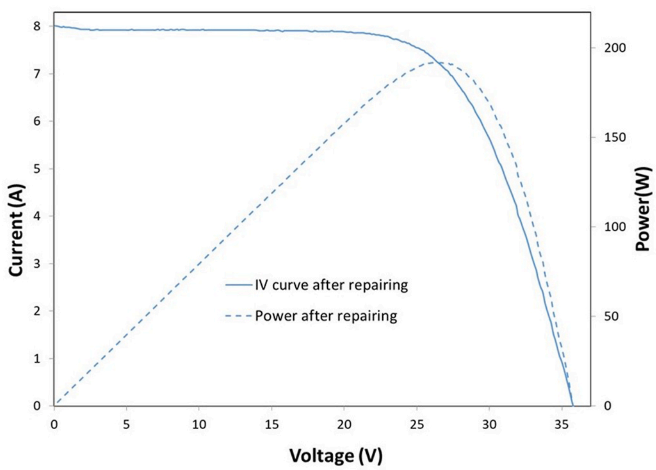

Fig. 20. Module M3 IV curves and power-voltage curves after repairing.

proposal by the same author. The second method is quite similar to ours, with a similar operational result, but it requires punching the modules backsheet in order to find interruptions. As mentioned before, these little holes can be a way for water, dust or other substances to penetrate the laminate and damage the EVA, cells and buses. This procedure can compromise the electrical insulation and safety of the module, immediately or in the future, in case the holes become a gateway for humidity, dust or any other undesirable element. The present work pays special attention to this issue, providing solutions that do not require punching the module backsheet. The work of [21], show a promising and elegant proposal, with an induction heating system solder. But it is used in modules specifically designed for the experiment, not in real modules. In our opinion this technique must be tested in the future in real modules. The paper of Kawano is not about locating interruptions, a key point in our work.

The main advantage of our proposal is the use of a non-aggressive, cheap, fast, accurate and an easy method for locating single and twin ribbon bus bar interruptions. Similarly, we have used quite conventional, intuitive and precise tools to repair them. Our proposal could facilitate the extension of repair to modestly equipped laboratories or factories, probably in countries were reduced labor cost made it economically interesting to repair modules in comparison with buying a

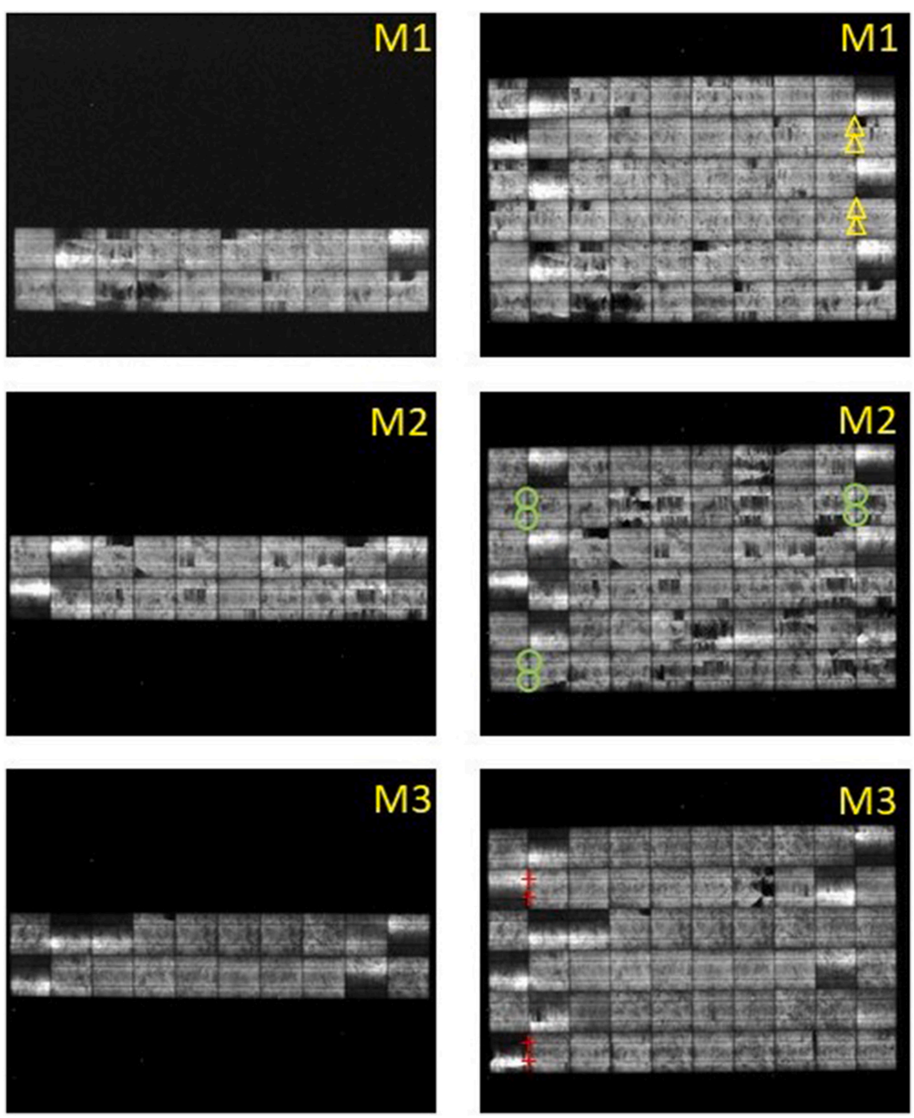

Fig. 21. EL images of each module before and after repairing. Modules before repairing are at left, modules after repairing at right. In the modules repaired, yellow triangles, green circles and red crosses mark the ribbon bus bars that were repaired.

new one.

4. Conclusions and future works

We propose that intercell electrical interruptions must be classified in single and twin ribbon bus bar interruption.

This paper proposes a fast, simple and cheap method for finding and repairing single and twin ribbon bus bar interruptions and the consequent failure in PV modules. This methodology can be applied in modestly equipped factories or laboratories, lowering the economic cost of repairing PV modules.

It is proposed to use a simple check in PV module, consisting of measuring the voltage at the electric contact of the junction box to find failures that could correspond to twin ribbon bus bar interruptions.

The use of tone testers or cable locators permits the precise identification of the twin interrupted cell interconnection, without drilling into the back side of the module or using expensive and time-consuming techniques such as electroluminescence. A tone tester that can perform this task can cost as low as few more than two tens of euros. A similar result can be achieved by using a current detector to locate single bus bar cell interruptions, also at low cost and with a fast procedure.

The repairing of the interruption can be performed after a short period of training and requires conventional handicraft tools like mini rotary drill tools and accessories, particularly grit sanding band, together with conventional soldering tools. A soldering paste and ribbon bus bar complements prove to be a good option for repairing the ribbon bus bar interruptions.

Fluid silicone can be used for the final insulation of the module, as has been done previously by other author for the restauration of damaged PV module backsheet. The dry and wet PV module insulation test is surpassed when using this simple solution.

Future works and improvements include:

- Testing the behavior of the repaired modules in a real installation.
- Extending the techniques to locate single ribbon bus bar interruptions using DC current or direct exposure to sunlight, by low-cost techniques and the study of the convenience of their repairing.
- Improve the soldering of interrupted ribbon bus bars.
- Improvement of backsheet sealing, restoration using EVA, backsheet and microlamination. Evaluation of alternative materials for EVA and backsheet repairing.

CRediT authorship contribution statement

Félix G. Rosillo: Conceptualization, Data curation, Formal analysis, Investigation, Methodology, Software, Supervision, Validation, Visualization, Writing – original draft, Writing – review & editing. **Maria Beatriz Nieto-Morone:** Investigation, Methodology, Supervision, Writing – review & editing. **Josue Benavides Esteva:** Investigation. **Felipe Soriano:** Investigation. **Sergio Temprano:** Investigation. **Claudia González:** Investigation, Methodology, Writing – review & editing. **María del Carmen Alonso-García:** Data curation, Formal analysis, Funding acquisition, Investigation, Methodology, Project administration, Resources, Supervision, Validation, Writing – original draft, Writing – review & editing.

Declaration of competing interest

The authors declare that they have no known competing financial interest or personal relationships that could have appeared to influence the work reported in the paper.

Acknowledgements

This work is part of the grant PID2020-118417RB-C21 funded by MICIN/AEI/10.13039/501100011033.

References

[1] P.P. Alves Dias, Raw Materials Demand for Wind and Solar PV Technologies in the Transition towards a Decarbonised Energy System, Publications Office. European Commission, Joint Research Centre, 2020.
[2] H.O.S. Mirletz, Circular economy priorities for photovoltaics in the energy transition, PLoS One 17 (9) (2022) e0274351, https://doi.org/10.1371/journal.pone.0274351.
[3] A.C. Norgren, Design for recycling principles applicable to selected clean energy technologies: crystalline-silicon photovoltaic modules, electric vehicle batteries, and wind turbine blades, J. Sustain. Metall. 6 (2020) 761–774.
[4] N.L. Rong Deng, A techno-economic review of silicon photovoltaic module recycling, Renew. Sustain. Energy Rev. 109 (2019) 532–550.
[5] M.B. Nieto-Morone, C.-G.-G. M, State and prospects of photovoltaic module waste generation in China, USA, and selected countries in Europe and South America, Sustain. Energy Fuels 7 (2023) 2163–2177.
[6] N.N. Francisco Prieto-Castrillo, Warranty assessment of photovoltaic modules based on a degradation probabilistic model, Prog. Photovoltaics Res. Appl. 28 (2020) 1308–1321.
[7] J.-S.L. Keiichi Komoto, End of life Management of Photovoltaic Panels: Trends in PV Module Recycling Technologies, International Energy Agency, 2018.
[8] M.S.K. Köntges, Review of Failures of Photovoltaic Modules, International Energy Agency, 2014.
[9] A.S. Michele Cândida Carvalho de Oliveira, The causes and effects of degradation of encapsulant ethylene vinyl acetate copolymer (EVA) in crystalline silicon photovoltaic modules: a review, Renew. Sustain. Energy Rev. (2018) 2299–2317.
[10] C. Dirk, T.J. Jordan, Photovoltaic failure and degradation modes, Prog. Photovoltaics Res. Appl. 25 (2017) 318–326.
[11] M.A. Munoz, A.-G. M, Early degradation of silicon PV modules and guaranty conditions, Sol. Energy (2011) 2264–2274.
[12] I.C. Elizabeth Markert, Private and externality costs and benefits of recycling crystalline silicon (c-Si) photovoltaic panels, Energies 2020 (2020) 3650.
[13] S.Y. Jing Tao, Review on feasible recycling pathways and technologies of solar photovoltaic modules, Sol. Energy Mater. Sol. Cell. 141 (2015) 108–124.
[14] A.C. Julien Walzberg, Role of the social factors in success of solar photovoltaic reuse and recycle programmes, Nat. Energy 6 (2021) 913–924.
[15] K. Lee, S. Cho, J.H. Yi, Simplified recovery process for resistive solder bond (RSB) hotspots caused by poor soldering of crystalline silicon photovoltaic modules using resin, Energies 15 (2022) 4623.
[16] G.C. Yuliya Voronko, Repair options for PV modules with cracked backsheets, Energy Sci. Eng. 9 (Issue 9) (2021) 1583–1595.
[17] G.E. Guy Beaucarne, Repair and preventive maintenance of photovoltaic module with degrading backsheets using flowable silicone sealant, Prog. Photovoltaics Res. Appl. (2021) 1–9.
[18] C. Gabriele, Y.V. Eder, Error analysis of aged modules with cracked polyamide backsheets, Sol. Energy Mater. Sol. Cell. 203 (2019).
[19] T.L. Curtis, Solar Photovoltaic Module Recycling: A Survey of U.S. Policies and Initiatives, National Renewable Energy Laboratory, 2021.
[20] A. Garvin, T.J. Heath, Research and development priorities for silicon photovoltaic module recycling to support a circular economy, Nat. Energy (2020) 502–510.
[21] Y. Kawano, J. Chantana, Y. Kuroda, K. Hirose, T. Minemoto, Development of repairing technique for interconnection of silicon photovoltaic modules using an induction heating system, Sol. Energy. 261 (2023) 55–62.
[22] Solarserver. (2006). https://www.solarserver.de/2006/08/04/photovoltaik-city-solar-gruppe-baut-derzeit-weltgroesstes-solar-kraftwerk-in-spanien.
[23] UNE, UNE-EN IEC 61215-2, Asociación Española de Normalización, 2021.
[24] Antonio, J. (2021). https://www.youtube.com/watch?v=ROBo3dJTRXs.
[25] A.V.-M. Eleonora Annigoni, Quantifying and modeling the impact of interconnection failures on the electrical performance of crystalline silicon photovoltaic modules, Prog. Photovoltaics Res. Appl. 27 (2019) 424–432.
[26] K. Lee, S. Cho, J. Yi, H. Chang, Prediction of power output from a crystalline silicon photovoltaic module with repaired cell-in-hotspots, Electronics 11 (2022) 2307.